

Efficient Adaptive Ensembling for Image Classification

Antonio Bruno[†], Davide Moroni^{†,*}, Massimo Martinelli[†]

Via Moruzzi 1, Pisa, Italy

Institute of Information Science and Technologies (ISTI) / National Research
Council of Italy (CNR)

[†] *These authors have contributed equally to this work and share first authorship*

Abstract

In recent times, except for sporadic cases, the trend in Computer Vision is to achieve minor improvements over considerable increases in complexity.

To reverse this tendency, we propose a novel method to boost image classification performances without an increase in complexity.

To this end, we revisited *ensembling*, a powerful approach, not often adequately used due to its nature of increased complexity and training time, making it viable by specific design choices. First, we trained end-to-end two EfficientNet-b0 models (known to be the architecture with best overall accuracy/complexity trade-off in image classification) on disjoint subsets of data (i.e. bagging). Then, we made an efficient adaptive ensemble by performing fine-tuning of a trainable combination layer. In this way, we were able to outperform the state-of-the-art by an average of 0.5% on the accuracy with restrained complexity both in terms of number of parameters (by 5-60 times), and Floating point Operations Per Second (by 10-100 times) on several major benchmark datasets, fully embracing the *green AI*.

Keywords: Deep Learning, Ensemble, Convolutional Neural Networks,

*Corresponding author

Email address: davide.moroni@isti.cnr.it (Institute of Information Science and Technologies (ISTI) / National Research Council of Italy (CNR))

URL: www.isti.cnr.it (Institute of Information Science and Technologies (ISTI) / National Research Council of Italy (CNR))

^{1†}.

1. Introduction

1.1. Motivations

Computer vision is one of the fields that most benefit from deep learning, continuously improving the state-of-the-art (SOTA) using Convolutional Neural
5 Networks (CNNs). In nearly all computer vision scenarios, complexity grows exponentially even for minimal improvements, both in terms of the number of parameters and in Floating point Operations Per Second (FLOPS). Table 1 briefly shows the evolution of the SOTA on the ImageNet classification task. It can be observed that the trend of improvements achieved only through high
10 complexity growth was temporarily slowed down by the introduction of EfficientNet architecture (and in particular with EfficientNet-b0 attaining the best accuracy/complexity trade-off). The previous also applies to other image classification (e.g. CIFAR) and computer vision tasks based on CNNs (e.g. object detection and segmentation).

15 1.2. Ensembling

Ensembling is the technique that combines several models, called *weak* learners, in order to produce a model with better performance than any of the weak learners alone [9, 10, 11]. Usually, the combination is accomplished by aggregating the output of the weak learners generally by voting (resp. averaging)
20 for classification (resp. regression). Other aspects, such as ensemble size (i.e. number of weak learners) and ensemble techniques (e.g. bagging, boosting, stacking), are crucial for obtaining a satisfactory result. Since it requires the training of several models, ensembles make the overall validation much more expensive, and model complexity grows at least linearly with respect to the ensemble size; moreover, ensembling is a time-consuming process, and this is the
25 main reason preventing a more extended use in practice, especially in Computer Vision. By converse, this work shows our technique to exploit this powerful tool

Model	Year	Accuracy	Parameters	FLOPs
AlexNet [1]	2012	63.3%	$\approx 60\text{M}$	$\approx 0.7\text{G}$
InceptionV3 [2]	2015	78.8%	$\approx 24\text{M}$	$\approx 6\text{G}$
ResNeXt-101 64x4 [3]	2016	80.9%	$\approx 84\text{M}$	$\approx 16\text{G}$
EfficientNet-b0 [4]	2019	77.1%	$\approx 5.3\text{M}$	$\approx 0.4\text{G}$
EfficientNet-b7 [4]	2019	84.3%	$\approx 67\text{M}$	$\approx 37\text{G}$
Swin-L [5]	2021	87.3%	$\approx 197\text{M}$	$\approx 103\text{G}$
NFNet-F4+ [6]	2021	89.2%	$\approx 527\text{M}$	$\approx 215\text{G}$
ViT-G/14 [7]	2021	90.45%	$\approx 1843\text{M}$	$\approx 965\text{G}$
CoAtNet-7 [8]	2021	90.88%	$\approx 2440\text{M}$	$\approx 2586\text{G}$

Table 1: Evolution of the state-of-the-art on the ImageNet classification task: as can be seen, complexity in models having accuracy $> 80\%$ (both in the number of parameters and FLOPs) grows exponentially in spite of a minimal improvement. The same trend can be noticed on other computer vision tasks. *N.B. only some architectures providing relevant improvements are shown in this table.*

with restrained resources (e.g. with respect to model complexity, validation time and training time).

30 1.3. Content outline

This work shows how applying a well-defined ensembling strategy using an efficient basic model as the core can improve the state-of-the-art in Computer Vision tasks, preserving a competitive performance/complexity trade-off. In Section 2 we describe our designing strategy in detail (e.g. model, ensembling
35 strategy, validation), focusing on introducing the main novel aspects. Experimental results and data description are shown in Section 3, while an exhaustive discussion is provided in the last section.

2. Efficient Adaptive Ensembling

2.1. Efficiency

At the foundations of the efficiency of the proposed method lies the basic core model adopted in this work: EfficientNet [4]. As the name suggests, EfficientNet improves the classification quality with lower complexity compared to models having similar classification performances. This is possible since EfficientNet performs optimised network scaling, given a predefined complexity. As shown in Figure 1, in the CNN literature, there are three main types of scaling:

- *depth scaling*, which consists in increasing the number of layers in the CNN; it is the most popular scaling method in the literature and allows detecting features at multiple levels of abstraction;
- *width scaling*, which consists in increasing the number of convolutional kernels and parameters or channels, giving the model the capability to represent different features at the same level;
- *input scaling*, represented by the increase in size/resolution of the input images, which allows capturing additional details.

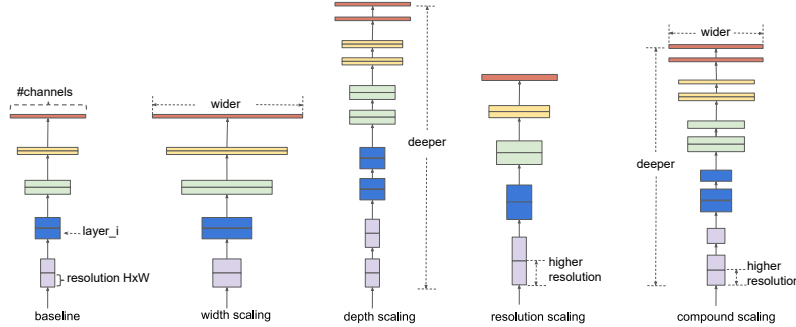


Figure 1: Example of scaling types, from left to right: a baseline network example, conventional scaling methods that only increase one network dimension (width, depth, resolution) and, at the end, the EfficientNet compound scaling method that uniformly scales all three dimensions with a fixed ratio. Image taken from the original paper [4].

Each of these scalings can be manually set or by a grid search. However, they increase the model complexity, usually exponentially, with tons of new parameters to tune and, after a certain level, scaling appears not to improve performances. The scaling method introduced in [4] is named *compound scaling*. It suggests that strategically performing all scaling together delivers better results because it is argued that they are dependent. Intuitively, they introduce the *compound coefficient* ϕ representing the amount of resources available to the model and find the optimal scaling combination given such a constrain, following the rules in the Equation 1. In this way, the total complexity of the network is approximately proportional to 2^ϕ (see the original paper for more details).

$$\begin{aligned} \text{depth: } d &= \alpha^\phi & \text{width: } w &= \beta^\phi & \text{resolution: } r &= \gamma^\phi \\ \text{such that } \alpha \cdot \beta^2 \cdot \gamma^2 &\approx 2 & \text{and } \alpha \geq 1, \beta \geq 1, \gamma \geq 1 \end{aligned} \quad (1)$$

2.2. Adaptivity

55 The adaptivity is given by the fact that the ensembling is data-driven and not fixed as usual. The typical way of combining weak learners is to perform voting/averaging as shown in Figure 2 (predicting the output from all weak learners and then picking the most frequent output/average of outputs), respectively for classification/regression. However, in this case, the ensemble is only a
60 static aggregator. In this work, we opted for performing an adaptive combination. However, instead of combining the outputs (Figure 3) of the weak learners, we combine the features that the CNNs extract from the input (Figure 4). In this way, we further reduce the complexity of the ensemble without reducing its power and expressiveness. Indeed the combination layer is of the same type of
65 output layer as the weak learners (i.e. Linear + LogSoftmax), and keeping both would introduce redundancy. This can be seen as a fully-differentiable version of Gradient Boosting [12]. However, in this way, there is no reason to perform the tree decision traversal and ensemble is performed at features-level.

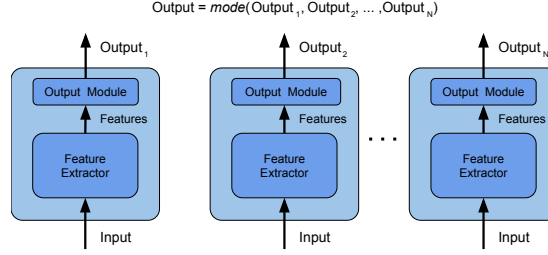


Figure 2: Ensemble by voting: the final output is obtained picking the mode among the output produced by the weak learners. In this way the weak learners are independent and it is effective with a high number of heterogeneous weak learners.

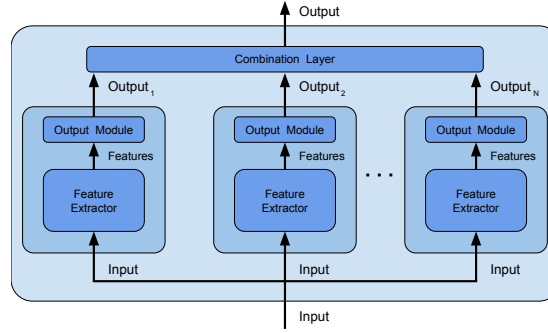


Figure 3: Ensemble by output combination: an additional combination layer is fed with the outputs of the weak learners and combines them. In this way the weak learners are no longer independent and the combination layer can be trained to better adapt to data.

3. Experimental results

70 In this section, the results obtained on several major benchmark datasets on image classification are described. Before showing the results, the main aspects of the experimental setup are detailed. The experiments have been implemented using the PyTorch [13] open-source machine learning framework.

3.1. Datasets

75 The proposed solution has been tested on several datasets in order to evaluate its capability of being effective over disparate domains (e.g. type of images, number of classes, balancing, quality) as shown in Table 2. A brief description

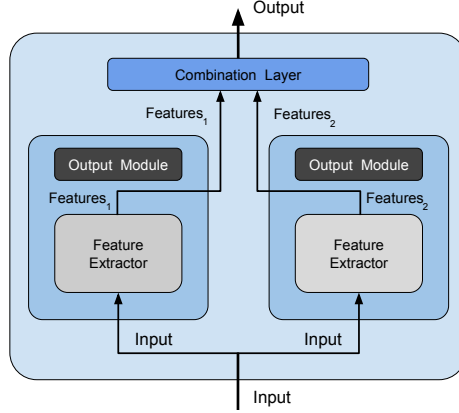


Figure 4: Our adaptive ensemble method: is an optimised version of the method shown in Figure 3 because we avoid redundancy and reduce complexity by deleting the output module (dark grey filled) of weak learners and feeding the combination layer with the features. Light grey filled modules denote modules whose parameters are frozen during training.

of each dataset follows:

CIFAR-10 and CIFAR-100 [14]: the CIFAR-10 dataset consists of 60000
 80 32×32 colour images in 10 classes, with 6000 images per class. There are 50000
 training images and 10000 test images.

This CIFAR-100 dataset is just like the CIFAR-10, except it has 100 classes
 containing 600 images each. There are 500 training images and 100 testing
 images per class. The 100 classes in the CIFAR-100 are grouped into 20 super-
 85 classes. Each image comes with a “fine” label (the class to which it belongs)
 and a “coarse” label (the superclass to which it belongs). In the experiments,
 the fine-grained version with 100 classes has been used.

Stanford Cars [15]: the Stanford Cars dataset contains 16185 360×240 colour
 90 images of 196 classes of cars at the level of *Make*, *Model*, *Year* (e.g. Tesla, Model
 S, 2012). The data is split into 8144 training images and 8041 testing images,
 where each class has been divided roughly in a 50-50 split. Since now, this
 dataset is referred as “Cars”.

95 **Food-101 [16]:** the Food-101 dataset consists of 101 food categories with 750 training and 250 test manually-reviewed images per category, making a total of 101000 images. On purpose, the training images contain some amount of noise that comes mainly in the form of intense colours and sometimes wrong labels. All images were rescaled to have a maximum side length of 512 pixels.

100

Oxford 102 Flower [17]: the Oxford 102 Flower is an image classification dataset consisting of 102 flower categories, most of them being plants commonly occurring in the United Kingdom. Each class consists of between 40 and 258 images. The images have large scale, pose and light variations. In addition, there are categories that have significant variations within the category and several very similar ones. Since now, this dataset is referred as “Flower102”.

CINIC-10 [18]: CINIC-10 is a dataset for image classification consisting of 270000 32×32 colour images. It was compiled as a “bridge” between CIFAR-10 and ImageNet, taking 60000 images from the former and 210000 downsampled images from the latter. It is split into three equal subsets - train, validation, and test - each containing 90000 images.

Oxford-IIIT Pet [19]: the Oxford-IIIT Pet Dataset has 37 categories with roughly 200 images for each class representing dogs or cats (25 classes for dogs and 12 for cats). Different versions of the dataset can be used for image classification, object detection, or image segmentation. In particular, for the experimentation, the fine-grained version of the image classification task has been used (i.e. predict the particular breed of the animal in the image instead of just determining if it is a dog or a cat). The images have wide variations in scale, pose and lighting. Since now, this dataset is referred as “Pets”.

120

3.2. Input preprocessing

The models are not fed directly with the images provided by the datasets, but images are preprocessed to improve the performances. In particular the only

Dataset	Domain	Input size	Classes	Balanced	Provided splits
CIFAR-10	Mixed (RGB)	32×32	10	Yes	Train-Test
CIFAR-100	Mixed (RGB)	32×32	100	Yes	Train-Test
Cars	Cars (RGB)	360×240	196	Yes	Train-Test
Food-101	Food (RGB)	512 larger side	101	No	Train-Test
Flower102	Flowers (RGB)	Various	102	Yes	Train-Valid-Test
CINIC-10	Mixed (RGB)	32×32	10	Yes	Train-Valid-Test
Pets	Dogs & Cats (RGB)	Various	37	Yes	Train-Valid-Test

Table 2: Details about the datasets used in the experiments.

two preprocessing step done are resize (size chosen after a preliminary tests) and normalization (in order to have all data of the same dataset described under the same distribution with pixel values in $[0, 1]$ range and centred around the mean) which improves stability and convergence of the training. Preprocessing details for each dataset are shown in Table 3. Even if augmentation has been performed on work representing the SOTA, no augmentation is performed in this work to test the performances of the “pure” method.

Dataset	Input size	Means (R,G,B)	Stds (R,G,B)
CIFAR-10	256×256	(0.491, 0.482, 0.447)	(0.246, 0.243, 0.261)
CIFAR-100	256×256	(0.507, 0.486, 0.441)	(0.267, 0.256, 0.276)
Cars	500×500	(0.468, 0.457, 0.450)	(0.295, 0.294, 0.302)
Food-101	500×500	(0.550, 0.445, 0.344)	(0.271, 0.275, 0.279)
Flower102	500×500	(0.433, 0.375, 0.285)	(0.296, 0.245, 0.269)
CINIC-10	256×256	(0.478, 0.472, 0.430)	(0.242, 0.238, 0.258)
Pets	500×500	(0.481, 0.448, 0.394)	(0.269, 0.264, 0.272)

Table 3: Input sizes and normalization values, for each channel, used for data preprocessing.

3.3. Transfer learning

Transfer learning [20] is the technique of taking knowledge gained while solving one problem, and applying it to a different but related problem. Like
135 the most cases for image classification, the stored knowledge is brought by pre-trained models from ImageNet [21] task, since it has more than 14 million images belonging to 1000 generic classes. Transfer learning has been used for weak learners training only.

3.4. Validation phases

140 Validation is divided into 2 main phases:

- end-to-end weak learner overfitting training: transfer learning starting from the ImageNet pre-trained model and setting a new output module (to fit the output size). The models are trained to reach overfit in order to get high specialization;
- 145 • ensemble combination layer fine-tuning: as shown in Figure 4 the weak learners are frozen removing their output modules, so in this phase only the combination layer is trained.

Both phases are performed using AdaBelief [22] optimizer which guarantees both fast convergence and generalization. AdaBelief parameters used are the
150 following ones: learning rate $5 \cdot 10^{-4}$, betas (0.9, 0.999), eps 10^{-16} , using weight decoupling without rectify.

3.5. Avoid overfitting

In order to prevent overfitting (i.e. avoid the model being too specialized to data from the training set with poor performances on *unknown* data), we use
155 early stopping (i.e. stop training after no improvements on validation set after a certain number of epochs, called *patience*) during fine-tuning only.

3.6. Data Splitting

Every dataset is provided with the “official” train-test split that is used for the ensemble fine-tuning. On the other hand, for the end-to-end overfitting training of the weak learners we perform the following data split:

1. set the size N of the final ensemble model (i.e. the number of weak learners to ensemble), in particular for the experiments $N=2$ in order to have the minimum ensemble size;
2. randomly split the dataset into N equally sized and disjoint (i.e. each data belongs exactly only to 1 subset) subsets with stratification (i.e. preserving the class ratios within the subset). During the test exception has made for the Pets dataset, in which the 2 disjoint subsets were made only by cats and dogs, respectively;
3. for each subset, instantiate a weak learner and train it only on that subset (called as *bagging*), with overfitting. In this way every weak learner will be highly specialized only on a portion of data, this could sound self-defeating but [23] showed that it leads to qualitative ensemble, especially in the case of this work in which ensembling is adaptive. The choice to reach overfitting will reduce the overall validation time: with preliminary tests we noticed that EfficientNet-b0 and AdaBelief optimizer with overfitting training are powerful and will always converge to the same minimum point (very likely to be the global one, due to the fact that accuracy is 100% almost always) independently on the initialization. In this way, just 2 train runs (only one initialization for each weak learner) are sufficient for every dataset.

3.7. Loss and Metrics

Training Loss: due to the multiclass nature of all dataset tasks, the Cross-Entropy Loss (which exponentially penalizes differences between predicted and true values, expressed as probability of class belonging) is used. For this reason, the model output has a specified size depending on the dataset (i.e. number

of classes) and each element *output*[*i*] represents the probability that the input sample belongs to class *i*.

Validation and test metrics: for the validation set evaluation, we decided to use the Weighted F1-score because this takes into account both correct and wrong predictions (true/false positive/negative) and weighting allows to manage any imbalance of the classes (more representative classes have a greater contribution). On the other hand, to make comparisons with previous works on test set, we used the same metric, which is Accuracy (i.e. correct prediction/total set) in all cases.

3.8. Hyperparameters

Some hyperparameters have already been fixed in the previous sections (i.e. preprocessing size and normalization, optimizer parameters and ensemble size), to further reduce the total validation time other hyperparameters have been fixed:

- early stopping patience: 10 epochs;
- batch size: 55 (200 in the case of fine-tuning) and 200 (700 in the case of the fine-tuning) for the 500×500 and 256×256 images, respectively.

while, for the ensemble fine-tuning, 5 different random seeds are used. In this way, for each dataset, 2 end-to-end weak training (1 for each subset) and 5 fine-tuning ensemble training are performed.

4. Results and Discussion

In this section results of experiments are shown and discussed. Table 4 shows that our work improves the SOTA in all major benchmark datasets and as expected the highest improvements (> 0.5%) are obtained on the tasks which are not saturated (i.e. accuracy < 99%). These results gain more evidence when complexity is considered too: indeed Table 5 shows that our work (except for the case of C1N1C-10) has 5-60 times less total number of parameters and needs

10-100 times less FLOPs respect to the SOTA. Moreover, in terms of trainable parameters, since it performs the fine-tuning of a combination layer, our final
 215 solution has only about 100K parameters to train.

Dataset	SOTA accuracy	Our accuracy	Improvement
CIFAR-10 [24]	99.500%	99.612%	0.112%
CIFAR-100 [25]	96.080%	96.808%	0.728%
Cars [26]	96.320%	96.868%	0.548%
Food-101 [25]	96.180%	96.879%	0.699%
Flower102 [27]	99.720%	99.847%	0.127%
CINIC-10 [28]	94.300%	95.064%	0.764%
Pets [25]	97.100%	98.220%	1.120%

Table 4: Classification test accuracy comparison between SOTA and our work on datasets used during experiments.

Last but not least, we present below an analysis of computation time for a single task; let:

- T_{end} the time for a single end-to-end weak learner training;
- T_{fine} the time for a single fine-tuning ensemble model training;
- 220 • T_{fwd} the time for a single forward step;
- T_{back} the time for a single backward step, if subscripted it indicates the number of parameters involved;
- T_{upd} the time for a single optimization update step, if subscripted it indicates the number of parameters involved.

225 Then for a single task the total time needed is:

$$T = A \cdot T_{end} + B \cdot T_{fine} \quad (2)$$

Dataset	SOTA parameters	Our parameters	SOTA FLOPs	Our FLOPs
CIFAR-10 [24]	$\approx 632\text{M}$	$\approx 11\text{M}$ (100K)	$\approx 916\text{G}^\dagger$	$\approx 0.9\text{G}$
CIFAR-100 [25]	$\approx 480\text{M}$	$\approx 11\text{M}$ (100K)	$\approx 299\text{G}^*$	$\approx 0.9\text{G}$
Cars [26]	$\approx 54.7\text{M}$	$\approx 11\text{M}$ (100K)	$\approx 10\text{G}$	$\approx 0.9\text{G}$
Food-101 [25]	$\approx 480\text{M}$	$\approx 11\text{M}$ (100K)	$\approx 299\text{G}^*$	$\approx 0.9\text{G}$
Flower102 [27]	$\approx 277\text{M}$	$\approx 11\text{M}$ (100K)	$\approx 60\text{G}$	$\approx 0.9\text{G}$
CINIC-10 [28]	$\approx 8.1\text{M}$	$\approx 11\text{M}$ (100K)	$\approx 1\text{G}$	$\approx 0.9\text{G}$
Pets [25]	$\approx 480\text{M}$	$\approx 11\text{M}$ (100K)	$\approx 299\text{G}^*$	$\approx 0.9\text{G}$

\dagger Estimation based on similar architecture with similar number of parameters.

$*$ Estimation based on the same architecture but scaling FLOPs w.r.t. the number of parameters ratio.

Table 5: Complexity, both number of parameters and FLOPs, comparison between SOTA and our work on datasets used during experiments.

where in our case $A = 2$ since end-to-end training is performed once on each of the two disjoint subset and $B = 5$ because we performed fine-tuning ensemble training with five random initializations.

However, it is possible to perform in parallel the end-to-end trainings halving
230 the batch size and about take the half of the time, the same goes for the fine-tuning training running all in parallel, in this way the total time is:

$$T = T_{\text{end}} + T_{\text{fine}} \quad (3)$$

and considering that a training is made of forward+backward+update steps to all training data for several epochs:

$$T_{\text{end}} \propto T_{\text{fwd}} + T_{\text{back}} + T_{\text{upd}} \quad (4)$$

$$T_{\text{fine}} \propto K \cdot T_{\text{fwd}} + T_{\text{back}_{100k}} + T_{\text{upd}_{100k}} \lesssim T_{\text{fwd}} \quad (5)$$

the approximation in the Equation5 is done because backward and update
235 steps involve only a small fraction of the parameters, moreover the two weak

learners perform forward steps in parallel since they are independent (otherwise we should have $K = 2$). Putting together Equations 4 and 5, the total time is:

$$T \lesssim 2 \cdot T_{fwd} + T_{back} + T_{upd} \quad (6)$$

What said before, in terms of FLOPs is (considering only one input, just add the linear scaling factor for the training on the whole dataset):

$$F_{fwd} = F_{back} = 0.39 \text{ GFLOPs} \quad (7)$$

$$F_{upd} \approx 20 \cdot P \approx 0.1 \text{ GFLOPs} \quad (8)$$

240 the Equation 7 refers to FLOPs of EfficientNet-b0 architectures and the Equation 8 refers to FLOPs of AdaBelief update step where $P = 5\text{M}$ is the number parameters involved in the end-to-end training. Putting all together:

$$\begin{aligned} F &\approx 2 \cdot F_{fwd} + F_{back} + F_{upd} \approx \\ &\approx 2 \cdot 0.39 + 0.39 + 0.1 \approx \\ &\approx 1.3 \text{ GFLOPs} \end{aligned} \quad (9)$$

this means that the *whole pipeline on a single image* requires about 1.3 GFLOPs, and considering the Table 5, the SOTA for CINIC-10 in [28] that has 245 least number of parameters (8.1M) requires requires 1 GFLOPs for *one single forward on an image*, showing that our solution is the fastest and the speedup is much more noticeable (10-100 times) over the even more complex SOTA models.

5. Conclusion and future works

In this work, we presented a method to reverse the trend in image clas- 250 sification of having minor improvements with a huge complexity increase. In particular, we showed a revisited *ensembling* to outperform the SOTA with restrained complexity, both in terms of numbers of parameters and FLOPs. Specifically, we proved how it is possible to perform bagging on two disjoint

subsets of data using two EfficientNet-b0 weak learners and training them to
255 overfit on the assigned/scheduled subset.

In this work we pushed the ensemble size to the lower bound using only 2
weak learners: this adaptive ensemble strategy would still be the most efficient
using up to 5 weak learners, and then it could be further improved by defining
different bagging strategies (e.g. train weak learners on subsets split by class
260 dimensionality, clustering or different color space mapping of inputs).

Then, the ensemble is performed by fine-tuning a trainable combination
layer. The efficiency of the method is given by different reasons: efficiency of
EfficientNet-b0 models, fine-tuning for ensemble and the high parallelization
capability of the solution. The reduced number of FLOPs combined with the
265 tiny validation space (7 total runs: 2 end-to-end + 5 fine-tuning) fully embraces
the idea of the green AI [29].

These results pave to investigate this kind of strategy in many fields: on
Object Detection (performing the ensemble at feature extraction backbone level)
and Segmentation (performing the ensemble on the encoding in typical encoder-
270 decoder architectures).

References

- [1] A. Krizhevsky, I. Sutskever, G. E. Hinton, Imagenet classification with deep
convolutional neural networks, *Communications of the ACM* 60 (2012) 84
– 90.
- 275 [2] C. Szegedy, V. Vanhoucke, S. Ioffe, J. Shlens, Z. Wojna, Rethinking the
inception architecture for computer vision, in: *2016 IEEE Conference on
Computer Vision and Pattern Recognition (CVPR)*, 2016, pp. 2818–2826.
`doi:10.1109/CVPR.2016.308`.
- [3] S. Xie, R. Girshick, P. Dollár, Z. Tu, K. He, Aggregated residual transfor-
280 mations for deep neural networks, in: *2017 IEEE Conference on Com-
puter Vision and Pattern Recognition (CVPR)*, 2017, pp. 5987–5995.
`doi:10.1109/CVPR.2017.634`.

- [4] M. Tan, Q. Le, EfficientNet: Rethinking model scaling for convolutional neural networks, in: K. Chaudhuri, R. Salakhutdinov (Eds.), Proceedings of the 36th International Conference on Machine Learning, Vol. 97 of Proceedings of Machine Learning Research, PMLR, 2019, pp. 6105–6114.
- [5] Z. Liu, Y. Lin, Y. Cao, H. Hu, Y. Wei, Z. Zhang, S. Lin, B. Guo, Swin transformer: Hierarchical vision transformer using shifted windows, CoRR abs/2103.14030 (2021). [arXiv:2103.14030](https://arxiv.org/abs/2103.14030).
URL <https://arxiv.org/abs/2103.14030>
- [6] A. Brock, S. De, S. L. Smith, K. Simonyan, High-performance large-scale image recognition without normalization, CoRR abs/2102.06171 (2021). [arXiv:2102.06171](https://arxiv.org/abs/2102.06171).
URL <https://arxiv.org/abs/2102.06171>
- [7] X. Zhai, A. Kolesnikov, N. Houlsby, L. Beyer, Scaling vision transformers, ArXiv abs/2106.04560 (2021).
- [8] Z. Dai, H. Liu, Q. V. Le, M. Tan, Coatnet: Marrying convolution and attention for all data sizes, CoRR abs/2106.04803 (2021). [arXiv:2106.04803](https://arxiv.org/abs/2106.04803).
URL <https://arxiv.org/abs/2106.04803>
- [9] D. W. Opitz, R. Maclin, Popular ensemble methods: An empirical study, J. Artif. Intell. Res. 11 (1999) 169–198. [doi:10.1613/jair.614](https://doi.org/10.1613/jair.614).
URL <https://doi.org/10.1613/jair.614>
- [10] X. Dong, Z. Yu, W. Cao, Y. Shi, Q. Ma, A survey on ensemble learning, Frontiers of Computer Science 14 (08 2019). [doi:10.1007/s11704-019-8208-z](https://doi.org/10.1007/s11704-019-8208-z).
- [11] O. Sagi, L. Rokach, Ensemble learning: A survey, Wiley Interdisciplinary Reviews: Data Mining and Knowledge Discovery 8 (2018) e1249. [doi:10.1002/widm.1249](https://doi.org/10.1002/widm.1249).

- 310 [12] J. H. Friedman, Greedy function approximation: A gradient boosting machine, *Annals of Statistics* 29 (2000) 1189–1232.
- [13] A. Paszke, S. Gross, F. Massa, A. Lerer, J. Bradbury, G. Chanan, T. Killeen, Z. Lin, N. Gimelshein, L. Antiga, A. Desmaison, A. Kopf, E. Yang, Z. DeVito, M. Raison, A. Tejani, S. Chilamkurthy, B. Steiner, 315 L. Fang, J. Bai, S. Chintala, Pytorch: An imperative style, high-performance deep learning library, in: H. Wallach, H. Larochelle, A. Beygelzimer, F. d'Alché-Buc, E. Fox, R. Garnett (Eds.), *Advances in Neural Information Processing Systems* 32, Curran Associates, Inc., 2019, pp. 8024–8035.
- 320 URL <http://papers.neurips.cc/paper/9015-pytorch-an-imperative-style-high-performance-deep-learning-library.pdf>
- [14] A. Krizhevsky, V. Nair, G. Hinton, Cifar-10 (canadian institute for advanced research).
- 325 URL <http://www.cs.toronto.edu/~kriz/cifar.html>
- [15] J. Krause, M. Stark, J. Deng, L. Fei-Fei, 3d object representations for fine-grained categorization, in: *4th International IEEE Workshop on 3D Representation and Recognition (3dRR-13)*, 2013.
- URL http://ai.stanford.edu/~jkrause/cars/car_dataset.html
- 330 [16] L. Bossard, M. Guillaumin, L. Van Gool, Food-101 – mining discriminative components with random forests, in: *European Conference on Computer Vision*, 2014.
- URL https://data.vision.ee.ethz.ch/cvl/datasets_extra/food-101/
- 335 [17] M.-E. Nilsback, A. Zisserman, Automated flower classification over a large number of classes, in: *Indian Conference on Computer Vision, Graphics and Image Processing*, 2008.
- URL <https://www.robots.ox.ac.uk/~vgg/data/flowers/102/>

- [18] L. N. Darlow, E. J. Crowley, A. Antoniou, A. J. Storkey, Cinic-10 is not
 340 imagenet or cifar-10, ArXiv abs/1810.03505 (2018).
 URL <https://datashare.ed.ac.uk/handle/10283/3192>
- [19] O. M. Parkhi, A. Vedaldi, A. Zisserman, C. V. Jawahar, Cats and dogs, in:
 IEEE Conference on Computer Vision and Pattern Recognition, 2012.
 URL <https://www.robots.ox.ac.uk/~vgg/data/pets/>
- [20] K. Weiss, T. Khoshgoftaar, D. Wang, A survey of transfer learning, Journal
 345 of Big Data 3 (05 2016). doi:10.1186/s40537-016-0043-6.
- [21] J. Deng, W. Dong, R. Socher, L. Li, Kai Li, Li Fei-Fei, Imagenet: A large-
 scale hierarchical image database, in: 2009 IEEE Conference on Computer
 Vision and Pattern Recognition, 2009, pp. 248–255. doi:10.1109/CVPR.
 350 2009.5206848.
- [22] J. Zhuang, T. Tang, Y. Ding, S. Tatikonda, N. Dvornek, X. Papademetris,
 J. Duncan, Adabelief optimizer: Adapting stepsizes by the belief in ob-
 served gradients, Conference on Neural Information Processing Systems
 (2020).
- [23] P. Sollich, A. Krogh, Learning with ensembles: How over-fitting can be
 355 useful, in: Proceedings of the 8th International Conference on Neural In-
 formation Processing Systems, NIPS’95, MIT Press, Cambridge, MA, USA,
 1995, p. 190–196.
- [24] A. Dosovitskiy, L. Beyer, A. Kolesnikov, D. Weissenborn, X. Zhai, T. Un-
 360 terthiner, M. Dehghani, M. Minderer, G. Heigold, S. Gelly, J. Uszkoreit,
 N. Houlsby, An image is worth 16x16 words: Transformers for image recog-
 nition at scale, in: ICLR 2021: The Ninth International Conference on
 Learning Representations, 2021.
- [25] P. Foret, A. Kleiner, H. Mobahi, B. Neyshabur, Sharpness-aware minimiza-
 365 tion for efficiently improving generalization, in: 9th International Confer-

ence on Learning Representations, ICLR 2021, Virtual Event, Austria, May 3-7, 2021, 2021.

[26] T. Ridnik, E. Ben-Baruch, A. Noy, L. Zelnik-Manor, Imagenet-21k pre-training for the masses (2021). [arXiv:2104.10972](#).

370 [27] H. Wu, B. Xiao, N. Codella, M. Liu, X. Dai, L. Yuan, L. Zhang, Cvt: Introducing convolutions to vision transformers (2021). [arXiv:2103.15808](#).

[28] Z. Lu, G. Sreekumar, E. Goodman, W. Banzhaf, K. Deb, V. N. Boddeti, Neural architecture transfer, IEEE Transactions on Pattern Analysis and Machine Intelligence 43 (9) (2021) 2971–2989. [doi:10.1109/tpami.2021.3052758](#).
375

[29] R. Schwartz, J. Dodge, N. A. Smith, O. Etzioni, Green ai, Commun. ACM 63 (12) (2020) 54–63. [doi:10.1145/3381831](#).
URL <https://doi.org/10.1145/3381831>